Second Harmonic Generation Electric Field Triplet Interferometry for Absolute Phasing

Raiden Speelman,[†] Nicole M. Gonzalez,[†] Camille M. Bridgewater, and Franz M. Geiger*

Department of Chemistry, Northwestern University

2145 Sheridan Road, Evanston, IL 60202, USA

Abstract. We report second harmonic generation electric field triplet interferometry performed using three mutually coherent ultrafast pulses in a common path with controllable relative phases, namely the light fields of a sample signal (SI), a reference oscillator (RO), and a local oscillator (LO). The ROLO phase determined from the interference of the light fields produced by two quartz wafers is subtracted from the phase determined from the SIROLO interferogram to yield the signal phase, ϕ_{SI}. The new method also calibrates the measured SHG intensity from a given sample internally by sending the fundamental light field reflected from the sample into one of the quartz wafers in the ROLO element. The approach avoids having to exchange the sample against a reference material with a known $\chi^{(2)}$ value or known phase and accounts, on-the-fly, for situations where the reflected fundamental light field intensity changes with experimental conditions. The new method is successfully benchmarked against z-cut α-quartz, fused silica held at its point of zero charge, and hematite nanolayers in air, across three different interferometers. The approach should be applicable for other second-order nonlinear spectroscopies, such as vibrational or electronic sum frequency generation.

[†]These authors contributed equally to this work

* Corresponding Author: f-geiger@northwestern.edu

Second-order nonlinear spectroscopy is a powerful means to follow physical and chemical processes at interfaces.[1-3] Multiple reviews summarize various applications to interfaces between condensed matter with vacuum or air, such as the air:water interface (to name one prominent example),[4] or with other condensed matter, such as aqueous electrochemical interfaces (to name another).[5] The amplitude and phase encode into the effective second-order nonlinear susceptibility from which interfacial molecular orientation distributions and physical properties such as the surface potential can be derived.[6-11] Here, the key requirement is the interference of the optical field from the sample (the signal, SI) with another optical field (the local oscillator, LO) of the same optical frequency but with a relative phase controlled by a phase shifting unit (PSU, Scheme 1A). The SILO interferogram, which can be obtained using a variety of methods, is then used to extract the signal amplitude, E_{SI}, and phase, ϕ_{SI}, from which the physical and materials properties one seeks can be obtained with the appropriate optical models.[7,12-17] The primary advantage of the approach is that it enables absolute phase referencing at buried solid/liquid interfaces with high phase stability and accuracy within a single, unchanged optical configuration that eliminates the need for repeated reference measurements.

As phases are inherently relative, phase-resolved nonlinear optical measurements require that the sample phase be determined relative to a standard material with a known phase. Commonly used phase standards are z-cut α-quartz,[18] potassium dihydrogen phosphate,[19] metals such as gold[20] or platinum,[21] or poled polymers.[22] In a 1986 report by Eisenthal and co-workers of phase referencing the SHG response of a phenol-covered air:water interface, the aqueous sample was replaced by a quartz block whose SHG field was interfered against an LO from a thin quartz wafer placed on a translational stage to take advantage of the optical dispersion in air.[23] The difference in the phases from the two interferograms (SI_{sample}+LO vs SI_{quartz}+LO) was then the sample's SHG

phase, reported from replicate measurements to ±15°. This work set the standard for subsequent approaches, some of which were summarized by Stolle et al. in 1996.[24]

Obtaining the absolute sample phase at condensed matter interfaces has its own challenges. An LO-before-SI approach that we published in 2005[25] avoided the problems posed by temporal and optical dispersion of condensed matter interfaces but did not produce an absolute sample phase. More recent attempts[7,12] to obtain the absolute phase at a glass:water interface using a z-cut α-quartz crystal aligned along the x-axis[23,26] that we pressed against the glass sample in lieu of the solution phase proved unsuccessful: While the nonlinear optical interference fringes were readily observed, the fitted phases varied by 10s to 100s of degrees as we moved from one sample spot to the next, or from one sample assembly to the next, a problem that persisted even when we used index-matching fluid. We attribute this result to imperfect sample flatness and the resulting minute, curved gap between the glass and the quartz. We then realized that one should be able to measure the interferogram from a glass:air interface and take its fitted phase to be the absolute zero phase, given that glass is transparent and non-birefringent at the fundamental and SHG wavelength, so that $E_{SHG,glass}e^{i\phi,glass}$ = real, and thus $\phi_{glass:air} = 0°$ from first principles.[7,12,19] After filling the cell with water and recording a new interferogram, the difference of the two fitted phases yields the absolute phase of the glass:water interface. In a second method, we placed fused silica into a pH 2.5 aqueous solution to establish the point of zero charge for which the surface potential, Φ(0), should be minimized.[27] The SHG signal produced by this interface should again be purely real, given that fused silica and water are transparent and non-birefringent at the fundamental and SHG wavelength, and given that the potential-dependent third-order contribution to the nonlinear optical response,[28-30] $\chi^{(3)}\Phi(0)$, is minimized at the PZC.

While these approaches are somewhat practical, they are not sample–general and require a change to the sample (going from air:glass to water:glass) or knowing the PZC, which can cover a broad pH range for many materials[27] and may not be known for others. One ideally would like to have a direct method and obtain the absolute zero phase on-the-fly. To do so, we now add a second z-cut α-quartz wafer as a reference oscillator (RO) in line of sight of the detector and use it to record the interferogram with the SHG fields from the sample, the reference oscillator, and the local oscillator to obtain the SIROLO phase, ϕ_{SIROLO} (Scheme 1B). We thus introduce "SHG electric field triplet interferometry" as interferometry performed using three mutually coherent ultrafast pulses in a common path with controllable relative phases. We then block the sample SHG signal with a long-pass filter and record the interferogram with the RO and LO fields only to obtain the ROLO phase, ϕ_{ROLO}. As we will show below, the absolute sample SHG phase, ϕ_{SI}, is then given by

$$\phi_{\mathrm{SI}} = \phi_{\mathrm{SIROLO}} - \phi_{\mathrm{ROLO}} \quad (1)$$

A numerical simulation of the SIROLO and ROLO interference patterns, illustrating the effect of phase modulation introduced by the rotating fused silica window, is presented in Supplemental Information Note S1. Our spectrometer (Fig. 1), described in detail in the Methods section, is driven by a Flint Oscillator (100 fs, 1030 nm, 80 MHz, Light Conversion, FL1-02, 8W). As described in our prior work,[7,12-14] we employ an off-axis parabolic mirror and a time delay compensator (TDC) to minimize the spatial and temporal dispersion plaguing nonlinear optical studies of condensed matter interfaces. The TDC is removed for air:solid interfaces. We now produce the RO in a second 50 μm z-cut α-quartz wafer. The PSU, consisting of a 1 mm thin fused silica window on a motorized rotational stage, is placed between the RO and the LO source. By rotating the PSU angle relative to the beam propagation, we vary the path length of the fundamental

and SHG fields in the fused silica window that constitutes the PSU. Due to fused silica's optical dispersion, the SHG phase shifts by a known amount relative to the fundamental as the path length through the silica window changes, i.e., with rotation of the fused silica window. This approach is similar to the one in section 2c of Stolle et al. for SHG,[24] and Hore et al. for sum frequency generation,[31] but now adds the RO to produce the SIROLO pulse triplet interferogram. We also included an offset, a linear, and a parabolic term to account for the linear Fresnel equations, i.e. any dependence of the transmitted fundamental and second harmonic intensity on the PSU angle, and the resulting minor variations in beam triplet overlap and alignment at the detector.

To isolate the absolute signal phase (ϕ_{SI}), we first obtain ϕ_{SIROLO} from the SIROLO interferogram. Here, all three light fields (SI, RO, and LO) are detected as a function of PSU angle. The measured phase consists of the signal phase (ϕ_{SI}), the RO phase (ϕ_{RO}), the LO phase (ϕ_{LO}), and any phase shift resulting from the instrument response, Δ_{Ins}, all of which add up because they are scalar (always purely real-valued) angles[32] according to

$$\phi_{\mathrm{SIROLO}} = \phi_{\mathrm{SI}} + [\phi_{\mathrm{RO}} + \phi_{\mathrm{LO}} + \Delta_{\mathrm{Ins}}] \quad (2)$$

We then define $[\phi_{\mathrm{RO}} + \phi_{\mathrm{LO}} + \Delta_{\mathrm{Ins}}] = \phi_{\mathrm{ROLO}}$ and determine it by blocking the sample SHG signal with a long-pass filter, allowing only the RO and LO to be detected as a function of PSU angle. Finally, we isolate ϕ_{SI} according to eqn. 1, test it as described next.

Our first experiment to test eqn. 2 used z-cut α-quartz, which has a well-known purely imaginary bulk SHG response whose phase is shifted 90º from the surface when properly aligned relative to the plane of incidence.[23,33] In external reflection, the SHG responses from the surface and the bulk mix, depending on the input angle. The resulting interference results in a mix of the 0º or 180º phase shift from the quartz surface, depending on the azimuthal angle,[18,28] and the 90º phase shift from the bulk, making the phase determination ambiguous.[34,35] We therefore accessed

quartz bulk SHG response by lining up the spectrometer on the back reflection from a 1 cm thick quartz block and sending the external reflection from the surface and its SHG signal to a beam block. The quartz block was placed on a motorized rotational stage to determine the angle of its maximum SHG response in the *s*-in/*p*-out polarization combination (50 mW input power). At this rotational angle, the quartz crystal is aligned with its crystallographic x-axis n·60° from the plane of incidence, where n is an integer (Fig. 2A). Every 60°, one crosses the crystallographic axis and the phase of quartz' bulk SHG response flips by 180°.[36] Azimuthal rotation revealed asymmetries in the expected periodic response of the quartz that depended on the sample equatorial angle and alignment of the instrument. To minimize the effect of the sample's equatorial angle, we align through the center of three reference points: the iris after the sample, the center of the RO quartz wafer, and the center of the LO quartz wafer. We minimized the asymmetries through iterative alignment of the sample and adjustments to the equatorial angle. Once minimized, we found the SHG maximum representing the x-axis of the z-cut quartz in the s-in p-out polarization combination. For the interferometry, we employ a 0.2 mm thick CaF_2 TDC (Newlight Photonics CAL12020-A) to account for the optical dispersion in bulk quartz.[37] Following eqn. 2, we determine ϕ_{SIROLO} from the interferogram of all three SHG light fields to be 58° ± 11°. The uncertainty in this point estimate is calculated from the average of three independent measurements in which we removed the quartz block from the sample stage after recording a set of SIROLO and ROLO fringes and then placed it back into the stage, followed by recording a new set of SIROLO and ROLO fringes. The fit error for a given SIROLO or ROLO fringe is <3°, improving with the S/N level and the number of PSU angle steps per fringe. We then block the sample SHG using a long-pass filter (Thorlabs FELH0850) to determine ϕ_{ROLO} to be 152° ± 3° (again from replicates obtained by removing and replacing the quartz block on the sample stage) and find the difference

to be -94° ± 14°, one of the cases of the ± 90° bulk quartz phases reported elsewhere (Fig. 2B; Table 1).[35,38] As shown in Supplemental Information Note S2, the measured phase flips between ± 90° every 60° of azimuthal angle rotation.

Encouraged by this result, we tested eqn. 2 further using a fused silica:water interface held at pH 2.5 (its point of zero charge).[39] For these experiments, a 1 mm thin fused silica window (Edmund Optics, 1λ, #19-837) was cleaned in Nochromix overnight, then sonicated in methanol and DIW for 15 minutes each, and plasma cleaned on "high" (Harrick) for two minutes. We used deionized water (DIW) from a MilliQ system (18.2 MΩ) that was lab air-equilibrated overnight to ensure a stable pH of ~5.8. The point of zero charge (PZC) of silica occurs at pH 2.5.[27] To prepare the solution, we used 1 M NaCl (Fisher, 99% purity, #223105) and adjusted the pH to 2.5 by adding HCl (Fisher Scientific, ACS Plus, Part #A144, 36.5−38.0%). In the experiments, we probed the interface in the internal reflection geometry for which we employed the 0.5 mm CaF_2 TDC as described earlier.[7,12-17] Due to the low SHG signal intensity from the silica:water interface (compared to the quartz block employed in the first test), 4 W input power was necessary to perform these measurements, as described in our recent work.[13,14] This input power leads to 2W at the fused silica:aqueous interface. The externally reflected 2W are blocked using an anodized aluminum beam block. We then rotated the RO and LO quartz wafer to angles that provide sufficiently high intensities that achieve interference, but not significantly higher than the sample intensity. A factor of 10:1 (ROLO:SI) is typical for fused silica:water samples.

In the experiment, we began by flowing DIW using a peristaltic pump set to 28 mL min^{-1} and recorded ten ROLO interference fringes for phase referencing. We then recorded the SIROLO fringes until the SHG phase and amplitude reached steady state, finding $\phi_{SI,DIW}$ = 15° ± 8° from three replicates. We then switched from DIW to the PZC solution (1 M NaCl, pH 2.5) and recorded

SIROLO fringes until the phase and amplitude again reached steady state. We concluded the experiment by recording another ten ROLO fringes. For the arguments given above, the SHG signal produced by this interface should be purely real. We find ϕ_{SIROLO} to be 135° ± 3° and ϕ_{ROLO} to be 134° ± 1° (three replicates), so that ϕ_{SI} is 1° ± 4° (Fig. 2C), close to the zero degrees expected for fused silica at the PZC.

Any instrument drift is readily accounted for in our method by alternating between the SIROLO and ROLO fringes. However, recording the ROLO fringes cuts the duty cycle in half. We therefore tested for instrument instability with a looped silica:DIW sample at a flow rate of 10 mL min^{-1} and found only negligible short- and long-term trends (Fig. 2E), as a linear least squares fit to the data yields an overall phase trend of just +0.005° ± 0.01° per hour over the 18-hour duration of the experiment. Certain 1-hour long time segments show drifts of 2° ± 1°. The amplitude remains stable, with an uncertainty of 3% over 18 hours. One can therefore safely record a ROLO fringe before and after a given experiment, provided the sample is not moved and that the spectrometer alignment is not changed. High-precision performance, however, will require alternating SIROLO:ROLO fringe measurements.

To demonstrate generality in terms of colored materials, we also determined the phase of an orange-colored 10 nm hematite nanolayer on fused silica to be 10° ± 1° (Fig. 2D, 150 mW input power), prepared as described elsewhere,[40] using three different spectrometers that we have now constructed in our laboratories. This result is consistent with the 515 nm SHG signal being in slight pre-resonance with hematite's optical absorption. Table 1 demonstrates that while each of the three spectrometers has its own ROLO phase, the SIROLO phases differ by the same amount for this sample. This result indicates that the ROLO element successfully accounts for each instrument's unique optical alignment. The standard deviation of ± 1° is taken from averaging the independently

determined sample phases obtained on the three spectrometers, as opposed to propagating the errors on each of the measurements.

In conclusion, we have presented a new second harmonic generation electric field triplet interferometer that employs the light fields of a sample signal, a reference oscillator, and a local oscillator. The ROLO phase determined from the interference of the light fields produced by two quartz wafers only is subtracted from the phase determined from the interferogram of the signal, the reference oscillator, and the local oscillator light fields (SIROLO) to yield the signal phase, according to $\phi_{SI} = \phi_{SIROLO} - \phi_{ROLO}$. The new method shortens the time required to carry out phase-resolved nonlinear optical experiments. It was validated through the 90° phase of bulk α-quartz and a near 0° phase obtained for fused silica at the PZC, consistent with zero net surface charge and interfacial potential. The approach opens the possibility of determining points of zero charge for other materials, including those used in electrochemical processes, where PZC determinations through differential capacitance measurements are challenging at the high ionic strength that is commonly used.[41,42]

As detailed in the Methods section, our second harmonic electric field triplet interferometer also internally calibrates the measured SHG intensity from a given sample by sending the fundamental light field reflected from the sample into one of the quartz wafers in the ROLO element. This approach avoids having to exchange the sample against a reference material with a known $\chi^{(2)}$ value, which would introduce optical misalignment. Our calibration procedure produces measured effective second-order nonlinear susceptibilities for the LO quartz wafer, $\chi^{(2)}_{LO,Eff}$, that are robust over more than one month of regular operation. While the common path approach is not necessary for the phase referencing, it is required for the intensity calibration. The procedure accounts for daily changes in alignment and for changes to a sample's optical properties

(transmission, reflectivity, absorption). This method also accounts, again on-the-fly, for situations where the reflected fundamental light field changes with experimental conditions, including variations in alignment, temperature, applied potential, stress, or photoillumination. Instrument stability in terms of SHG amplitude and phase was demonstrated over 18 hours. The approach should be applicable for other second-order nonlinear spectroscopies, such as vibrational or electronic sum frequency generation.[4,43]

Experimental Method.

Spectrometer. We use an Ytterbium crystal-based 8 W Flint oscillator (100 fs, Light Conversion) operating at a repetition rate of 80 MHz and a central wavelength of 1030 nm. Figure 1A depicts our PR-SHG spectrometer. First, we split the laser output using a 50/50 beam splitter (TP-OR-BS-R50, Light Conversion) and direct one of the beams into our spectrometer using beam routing mirrors (TP-OR-BRM, Light Conversion). The laser power is controlled using a variable attenuator (model 990-0076, Eksma Optics), after which unprotected gold mirrors (PF10-03-M03, Thorlabs) are used for beam propagation. A femtoline zero-order air-spaced half-wave plate (464-4208, Eksma Optics) is used to rotate the plane of polarization to be parallel to the laser table, corresponding to *s*-in polarization at the sample interface (which is perpendicular to the laser table). The waveplate is calibrated using a polarizer cube (GT15-B, Thorlabs). We then send the fundamental through a long-pass filter (FELH900, Thorlabs) to remove any residual SHG and then through an achromatic focusing lens with a 10 cm focal length to focus onto our sample (110-1211E+AR1030HT, Eksma).

The sample SHG and the reflected fundamental beam are then recollimated and spatially overlapped with an off-axis parabolic mirror (OAP, Thorlabs MPD149-P01). The beams then travel through a calcite time delay compensator (TDC, Newlight CAL12020-A or CAL12050-A)

to temporally overlap the fundamental and the SHG beams. A TDC is not necessary when recording interference fringes in external reflection, given the weak optical dispersion in air at 1030 and 515 nm.

After the TDC, the reflected fundamental and the sample signal (SI) beams travel through a 50 μm thin quartz wafer (PWQB-368252, Precision MicroOptics) where the RO field is produced. The fundamental, SI, and RO now travel through a phase shifting unit (PSU), which is a 1 mm thick silica glass window (Edmund Optics 11876) mounted onto a computer-controlled motorized rotational stage (ELL18K, Thorlabs). The three beams then travel through another 50 μm thin quartz wafer, which generates the LO field from part of the fundamental. The RO and LO quartz wafers are aligned as described in Supporting Information Note S2.

The phase of the LO field is modulated relative to the SIRO depending on the PSU angle. The four beams are then routed past two silver mirrors, through a polarizer analyzer (PA, Thorlabs GL15) to control the output polarization (set to *p*-out), and a band pass filter (Thorlabs FESH0850) to block any remaining fundamental light. The beams are then aligned into a photomultiplier tube (PMT, Hamamatsu H8259-01), where the SHG intensity resulting from the constructive/destructive interference of the SI, RO, and LO fields is recorded as a function of PSU angle. For the ROLO measurements, a long-pass filter (FELH900, Thorlabs) placed before the TDC is used to block any SHG generated by the sample. The following equation is used to fit the interferograms:

$$\mathrm{I_{SHG}} = \mathrm{K_0} + \mathrm{K_1}1(\theta - \Delta\theta) + \mathrm{K_2}(\theta - \Delta\theta)^2 + \mathrm{E_{Sig}}\cos\left\{4\pi\left(\frac{\delta_{\mathrm{PSU}}}{\lambda}\right)\right\}\cdot$$

$$\cdot\left\{\mathrm{n_{2\omega}}\cos\left(\arcsin\left(\sin\left(\frac{\theta - \Delta\theta}{\mathrm{n_{2\omega}}}\right)\right)\right)\right\} - \left\{n_\omega\, cos\left(arcsin\left(sin\left(\frac{\theta - \Delta\theta}{n_\omega}\right)\right)\right)\right\} + \phi_{\mathrm{SIROLO}} \quad (3)$$

Here, I_{SHG} is the measured SHG intensity, K_0 accounts for the intensity-offset of the interference pattern, K_1 accounts for the linear tilt and K_2 for the parabolic bend of the interference pattern, θ is the PSU angle, $\Delta\theta$ accounts for the minor offset in the PSU angle relative to the absolute zero-position on the rotational stage, E_{SI} is the SHG amplitude, δ_{PSU} is the thickness of the fused silica window (1.07566 mm), λ is the fundamental wavelength (1030 nm), $n_{2\omega}$ is the refractive index of the PSU for the SHG wavelength ($n_{2\omega}$=1.4619), n_{ω} is the refractive index of the PSU for the fundamental wavelength (n_{ω}=1.4501), and ϕ_{SIROLO} is the SHG phase relative to the LO from the resulting interference. This equation is adapted from eqn. 8 found in Stolle et al.,[24] but now includes parabolic bend and linear tilt. Each fringe takes 20 seconds to acquire, which includes resetting the motor to the starting position. We note that eqn. 1 follows a simple cosine function when expressed not as a function of the PSU rotational angle but of distance the light travels in the PSU's fused silica window at each rotational angle. We note that one of our three spectrometers was built as the mirror image of the layout shown in Fig. 1. The phases obtained from this particular spectrometer are therefore multiplied by -1, producing the same-signed ϕ_{SI} values for fused silica:PZC and our hematite samples.

Instrument Calibration Factor. The signal intensity recorded by SHG spectrometers depends on the detector sensitivity and the transmission/reflectivity of the various elements (mirrors, waveplates, lenses, quartz wafers, PSU). Slight changes in sample placement and focus can also influence the SHG signal intensity. To compare measurements carried out on different instruments, or to quantify sample-to-sample or day-to-day variations, a calibration factor must be employed. Previous work exchanges the target sample with a quartz sample in the same position, measures the input and output angles to determine the Fresnel factors, and then compares the target sample intensity to the quartz intensity.[7,12,16,44] This method requires exchanging the sample and precise

realignment. Our new approach utilizes the LO quartz wafer to internally calibrate the spectrometer without the need to realign or assume that the calibration factor remains constant over time.

To begin, we obtain the effective nonlinear susceptibility of the LO quartz wafer. To this end, we place our quartz block in place of the sample position onto a motorized rotational mount (Thorlabs K10CR1) and align the spectrometer on the external reflection, using the focus we found for the sample interface (say, the fused silica:water interface). We block the quartz block's internal reflection using a flag. For reasons given below, we set the input power, P_{In}, to 160 mW, use the 0.5 mm TDC we employ in our fused silica:water interface sample to account for its transmittance, flip the RO and LO quartz wafers out of the way, and move the PSU to 0°. We then rotate the quartz block azimuthally to one of the angles that yields maximum SHG intensity to measure I_{QB}. We then add our long-pass filter between the sample at the off-axis parabolic mirror, flip the LO quartz wafer into the beam path, and record the SHG intensity to measure I_{LO}. We then flip the LO quartz wafer out of the way and put a power meter in its place to record the power at the LO position, $P_{@LO}$, which reads 20 mW when using P_{In}=160 mW in our spectrometer (*n.b.*: higher input powers lead to $P_{@LO}$ that are too high, as evidenced by a departure from the expected quadratic power dependence of I_{LO}). $\boldsymbol{\chi^{(2)}_{LO,Eff}}$ is given as follows:

$$\chi^{(2)}_{LO,Eff} = \frac{|F_{QB}|}{|F_{LO}|}\frac{4d_{11}}{|\Delta k_z|}\frac{\sqrt{I_{LO}*\left(\frac{P_{In}}{P_{@LO}}\right)^2}}{\sqrt{I_{QB}}} \quad (4)$$

Here, F_{QB} is the Fresnel factor from the air:quartz block interface, F_{LO} is the Fresnel factor of the LO quartz wafer, d_{11} is the nonlinear coefficient for SHG of bulk quartz, and Δk_z is the wave vector mismatch for the air:quartz block interface. We calculate the Fresnel factors using the

equations described in Supplemental Information Note S3, taking the bulk quartz d_{11} to be 0.3 pm V^{-1} for s-in p-out polarization combination according to Boyd.[45]

The instrument calibration factor, C, is obtained as follows: We replace the quartz block with a fused silica window in contact with a pH 2.5 aqueous solution (silica's PZC) to produce a purely real SHG response. This interface requires a P_{In} of 4W in our spectrometer, denoted below as $P_{In,4W}$ = 4W. As discussed above, a fused silica or glass slide would also produce a purely real SHG response, but we found no difference in the ROLO vs SIROLO interference fringes in either external or internal reflection. This outcome is due to the fact that the SHG intensity from the sample only is several orders of magnitude smaller than that of the RO or LO quartz wafers. With the long-pass filter and the 0.5 mm TDC in place after the sample, the RO quartz wafer flipped out of the way, and the PSU angle set to 0°, we now measure the SHG intensity from the LO quartz wafer that is produced by the 1030 nm light reflected from the fused silica/PZC sample, $I_{LO,4W}$. We then calculate the effective power of the 1030 nm fundamental at the LO quartz wafer according to $P_{@LO,4W} = 20mW \cdot (I_{LO,\,4W}/I_{LO,\,20mW})^{1/2}$. The instrument's calibration factor for this input power of 4 W, C_{4W}, is then determined with the following equation:

$$C_{4W} = \frac{\sqrt{I_{SI,4W}}}{\sqrt{I_{LO,4W} * \left(\frac{P_{In,4W}}{P_{@LO,4W}}\right)^2}} * \frac{|F_{LO}|}{|F_{Sample}|} * \chi^{(2)}_{LO,Eff} \qquad (5)$$

Here, $I_{SI,4W}$ is the SHG intensity obtained with 4W input power, $I_{LO,4W}$ is the local oscillator intensity produced with that input power, F_{LO} and F_{Sample} are the LO quartz wafer's and the sample's Fresnel factors (see again Supplemental Note S3), and $\chi^{(2)}_{LO,Eff}$ is the effective second-order nonlinear susceptibility of the LO quartz wafer (eqn. 4). Combining eqn. 4 and 5 cancels F_{LO} so that it does not need to be quantified. One can now employ eqn. 5 to account, on-the-fly, for any

changes in the optical reflectivity of the sample at the fundamental by simply measuring the SHG intensity produced by the LO quartz wafer during a given experiment.

Supporting Information. Simulated interference patterns, RO and LO quartz wafer alignment procedure, bulk SHG phase quantification as a function of quartz block azimuthal angle, dependence of the SIROLO and ROLO phases on RO and LO quartz wafer translational position and TDC azimuthal angle alignment, computation of Fresnel coefficients.

Author Contributions. FMG conceived of the idea. All authors participated in the design and construction of the spectrometers described in this work and in the collection and analysis of data. RS, NMG, and FMG wrote the manuscript.

Acknowledgments. This work was supported by the US National Science Foundation (CHE-2153191, acknowledged for partial support of the oscillator and detection instrumentation, and CHE-2404203, acknowledged for support of NMG. NMG and RS also acknowledge support from Northwestern University's International Institute for Nanotechnology through an IIN Postdoctoral Fellowship and a Patrick G. and Shirley W. Ryan Fellowship, respectively. CMB acknowledges support from an NSF Graduate Research Fellowship. RS and FMG are also grateful for support by the U.S. Department of Energy, Office of Science, Office of Basic Energy Sciences, Chemical Science, Geosciences and Biosciences Division through grants DE-SC0023342 and DE-SC0026327. Partial support for the oscillator was also provided by the Sloan Foundation through grant G-2019-12300.

References

1. Eisenthal, K., Liquid interfaces probed by second-harmonic and sum-frequency spectroscopy. *Chem Rev* **1996,** *96* (4), 1343-1360.

2. Shen, Y. R.; Ostroverkhov, V., Sum-frequency vibrational spectroscopy on water interfaces: polar orientation of water molecules at interfaces. *Chemical Reviews* **2006,** *106* (4), 1140-1154.

3. Eisenthal, K. B., Second harmonic spectroscopy of aqueous nano-and microparticle interfaces. *Chemical Reviews* **2006,** *106* (4), 1462-1477.

4. Tang, F.; Ohto, T.; Sun, S.; Rouxel, J. R.; Imoto, S.; Backus, E. H.; Mukamel, S.; Bonn, M.; Nagata, Y., Molecular structure and modeling of water–air and ice–air interfaces monitored by sum-frequency generation. *Chemical Reviews* **2020,** *120* (8), 3633-3667.

5. Ge, A.; Rudshteyn, B.; Videla, P. E.; Miller, C. J.; Kubiak, C. P.; Batista, V. S.; Lian, T., Heterogenized molecular catalysts: vibrational sum-frequency spectroscopic, electrochemical, and theoretical investigations. *Accounts of Chemical Research* **2019,** *52* (5), 1289-1300.

6. Chang, H.; Lozier, E. H.; Ma, E.; Geiger, F. M., Quantification of Stern Layer Water Molecules, Total Potentials, and Energy Densities at Fused Silica:Water Interfaces for Adsorbed Alkali Chlorides, CTAB, PFOA, and PFAS. *The Journal of Physical Chemistry A* **2023,** *127* (40), 8404-8414.

7. Speelman, R.; Marker, E. J.; Boamah, M. D.; Kupferberg, J.; Bye, J. Z.; Engelhard, M.; Zhao, Y.; Martinson, A. B. F.; Rosso, K. M.; Geiger, F. M., Water flipping and the oxygen evolution reaction on Fe2O3 nanolayers. *Nat Commun* **2025,** *16* (1), 3585.

8. Speelman, R.; Marker, E. J.; Geiger, F. M., Quantifying Stern layer water alignment before and during the oxygen evolution reaction. *Science Advances* **2025,** *11* (10), eado8536.

9. Cai, C. Y.; Azam, M. S.; Hore, D. K., Determining the Surface Potential of Charged Aqueous Interfaces Using Nonlinear Optical Methods. *Journal of Physical Chemistry C* **2021,** *125* (45), 25307-25315.

10. Patterson, J. E., The nonresonant sum-frequency generation response: The not-so-silent partner. *The Journal of Chemical Physics* **2024,** *161* (6).

11. Hore, D. K., Phase of the second-order susceptibility in vibrational sum frequency generation spectroscopy: Origins, utility, and measurement techniques. *The Journal of Chemical Physics* **2024,** *161* (6), 060902.

12. Speelman, R. S.; Marker, E.; Geiger, F. M., Quantifying Stern Layer Water Alignment Prior to and During the Oxygen Evolution Reaction. *Science Advances* **2025,** *11*, eado8536.

13. Gonzalez, N. M.; Alghamdi, A. O.; Geiger, F. M., Dehydration of Oxide: Water Interfaces by Brines Quantified with Nonlinear Spectroscopy, in press. *J. Am. Chem. Soc.* **2025**.

14. Alghamdi, A. O.; Gonzalez, N. M.; Geiger, F. M., Temperature Dependence of Proton Coverage and the Total Potential at Fused Silica: Water Interfaces from Phase-Resolved Nonlinear Optics. *J. Am. Chem. Soc.* **2025,** *147* (17), 14308-14315.

15. Chang, H.; Lozier, E. H.; Ma, E.; Geiger, F. M., Quantification of Stern Layer Water Molecules, Total Potentials, and Energy Densities at Fused Silica:Water Interfaces for Adsorbed Alkali Chlorides, CTAB, PFOA, and PFAS. *J. Phys. Chem. A* **2023,** *127*, 8404-14.

16. Ma, E.; Ohno, P. E.; Kim, K.; Liu, Y.; Lozier, E. H.; Miller III, T. F.; Wang, H.-f.; Geiger, F. M., A New Imaginary Term in the 2nd Order Nonlinear Susceptibility from Charged Interfaces. *J. Phys. Chem. Lett.* **2021,** *12* (24), 5649-59.

17. Boamah, M. D.; Ohno, P. E.; Lozier, E.; Van Ardenne, J.; Geiger, F. M., Specifics about Specific Ion Adsorption from Heterodyne-Detected Second Harmonic Generation. *Journal of Physical Chemistry B* **2019,** *123* (27), 5848-5856.

18. Hu, X.-H.; Wei, F.; Wang, H.; Wang, H.-F., α-Quartz Crystal as Absolute Intensity and Phase Standard in Sum-Frequency Generation Vibrational Spectroscopy. *J. Phys. Chem. C* **2019,** *123*, 15071-86.

19. Chang, R.; Ducuing, J.; Bloembergen, N., Relative phase measurement between fundamental and second-harmonic light. *Physical Review Letters* **1965,** *15* (1), 6.

20. Covert, P. A.; Hore, D. K., Assessing the Gold Standard: The Complex Vibrational Nonlinear Susceptibility of Metals. *J. Phys. Chem. C* **2014,** *119*, 271-6.

21. Xu, P.; Huang, A.; Suntivich, J., Phase-Sensitive Second-Harmonic Generation of Electrochemical Interfaces. *J. Phys. Chem. Lett.* **2020,** *11*, 8216-21.

22. Nelson, C.; Luo, J.; Jen, A.-Y.; Laghumavarapu, R.; Huffaker, D.; Zhu, X.-Y., Time-, energy-, and phase-resolved second-harmonic generation at semiconductor interfaces. *The Journal of Physical Chemistry C* **2014,** *118* (48), 27981-27988.

23. Kemnitz, K.; Bhattacharyya, K.; Hicks, J. M.; Pinto, G. R.; Eisenthal, K. B.; Heinz, T. F., The Phase of 2nd-Harmonic Light Generated at an Interface and Its Relation to Absolute Molecular-Orientation. *Chem. Phys. Lett.* **1986,** *131* (4-5), 285-290.

24. Stolle, R.; Marowsky, G.; Schwarzberg, E.; Berkovic, G., Phase measurements in nonlinear optics. *Appl. Phys. B* **1996,** *63*, 491-498.

25. Mifflin, A. L.; Musorrafiti, M. J.; Konek, C. T.; Geiger, F. M., Second harmonic generation phase measurements of Cr (VI) at a buried interface. *J. Phys. Chem. B* **2005,** *109*, 24386-90.

26. Ohno, P. E.; Saslow, S. A.; Wang, H.-f.; Geiger, F. M.; Eisenthal, K. B., Phase-referenced nonlinear spectroscopy of the α-quartz/water interface. *Nat. Commun.* **2016,** *7*, 13587.

27. Kosmulski, M., The pH dependent surface charging and points of zero charge. X. Update. *Advances in Colloid and Interface Science* **2023,** *319*, 102973.

28. Ohno, P. E.; Saslow, S. A.; Wang, H.-f.; Geiger, F. M.; Eisenthal, K. B., Phase-referenced Nonlinear Spectroscopy of the alpha-Quartz/Water Interface. *Nat Commun* **2016,** *7*, 13587.

29. Gonella, G.; Lutgebaucks, C.; de Beer, A. G. F.; Roke, S., Second Harmonic and Sum-Frequency Generation from Aqueous Interfaces is Modulated by Interference. *J. Phys. Chem. C* **2016,** *120*, 9165-9173.

30. Wen, Y.-C.; Zha, S.; Liu, X.; Yang, S.; Guo, P.; Shi, G.; Fang, H.; Shen, Y. R.; Tian, C., Unveiling Microscopic Structures of Charged Water Interfaces by Surface-Specific Vibrational Spectroscopy. *Physical Review Letters* **2016,** *116* (1), 016101.

31. Covert, P. A.; FitzGerald, W. R.; Hore, D. K., Simultaneous measurement of magnitude and phase in interferometric sum-frequency vibrational spectroscopy. *The Journal of Chemical Physics* **2012,** *137* (1), 014201.

32. Born, M.; Wolf, E., *Principles of Optics, 7th ed.* Cambridge University Press: 2020.

33. Bloembergen, N.; Pershan, P. S., Light Waves at the Boundary of Nonlinear Media. *Physical Review* **1962,** *128*, 606.

34. Sun, S.; Liang, R.; Xu, X.; Zhu, H.; Shen, Y. R.; Tian, C., Phase reference in phase-sensitive sum-frequency vibrational spectroscopy. *J. Chem. Phys.* **2016,** *144*, 244711.

35. Thämer, M.; Garling, T.; Campen, R. K.; Wolf, M., Quantitative determination of the nonlinear bulk and surface response from alpha-quartz using phase sensitive SFG spectroscopy. *The Journal of Chemical Physics* **2019,** *151* (6).

36. Fu, L.; Chen, S.; Wang, H.-F., Validation of Spectra and Phase in Sub-1 cm-1 Resolution Sum-Frequency Generation Vibrational Spectroscopy Through Internal Heterodyne Phase Resolved Measurement. *The Journal of Physical Chemistry B* **2015**.

37. t1.

38. Sun, S.; Liang, R.; Xu, X.; Zhu, H.; Shen, Y. R.; Tian, C., Phase reference in phase-sensitive sum-frequency vibrational spectroscopy. *The Journal of Chemical Physics* **2016,** *144* (24).

39. Kosmulski, M., The pH dependent surface charging and points of zero charge. VI. Update. *Journal of Colloid and Interface Science* **2014,** *426*, 209-212.

40. Speelman, R.; Martin, L.; Bye, J.; Kupferberg, J.; Boamah, M.; Rosso, K.; Alex, M.; Geiger, F. M., Thickness Dependent Flat Band Potentials at the Nanoscale on Hematite Electrodes and an Alternative Fabrication to Atomic Layer Deposition, chemRxiv 10.26434/chemrxiv-2025-56l44. **2025**.

41. Bard, A. J.; Faulkner, L. R., *Electrochemical Methods: Fundamentals and Applications*. 2nd ed.; John Wiley and Sons: New York, 2000.

42. Xu, P.; von Rueden, A. D.; Schimmenti, R.; Mavrikakis, M.; Suntivich, J., Optical method for quantifying the potential of zero charge at the platinum-water electrochemical interface. *Nature Materials* **2023,** *22*, 503-10.

43. Raab, M.; Becca, J. C.; Heo, J.; Lim, C.-K.; Baev, A.; Jensen, L.; Prasad, P. N.; Velarde, L., Doubly resonant sum frequency spectroscopy of mixed photochromic isomers on surfaces reveals conformation-specific vibronic effects. *J. Chem. Phys.* **2019,** *150*, 114704.

44. Dalstein, L.; Chiang, K.-Y.; Wen, Y.-C., Direct Quantification of Water Surface Charge by Phase-Sensitive Second Harmonic Spectroscopy. *The Journal of Physical Chemistry Letters* **2019,** *10* (17), 5200-5205.

45. Boyd, R. W., *Nonlinear Optics: Third Edition*. Academic Press: London, 2008.

Table 1. Phases of different samples obtained using SHG pulse triplet interferometer. Numbers in parentheses represent the standard deviation of three replicates.

	Bulk Quartz	Silica:DIW	Silica:pH 2.5	Hematite:Air*
ϕ_{SIROLO}	58 (11)	149 (7)	135 (3)	137 (1), 62 (1), -92 (1)
ϕ_{ROLO}	152 (3)	134 (1)	134 (1)	128 (5), 53.9 (0.3), -103 (3)
ϕ_{SI}	-94 (14)	15 (8)	1 (4)	9 (6), 8 (1), 11 (4)

*From three different spectrometers.

Figure Captions.

Scheme 1. Pulses generated by the sample, reference oscillator, and local oscillator. (A) Previous SILO-based approach, in which the sample SHG field (SI) interferes with the local oscillator (LO) field, and the relative phase is obtained using a rotating phase shifting unit (PSU). (B) SIROLO approach incorporating an additional quartz wafer as the reference oscillator (RO), enabling direct determination of the absolute sample phase from the difference of the SIROLO and the ROLO phase.

Figure 1. Phase-Resolved Second Harmonic Generation Spectrometer and Extracting Phase from Wave mixing. Phase-resolved second harmonic generation spectrometer (PR-SHG) consisting of a long-pass filter (LPF), half-waveplate ($\boldsymbol{\lambda/2}$), variable density filter (VDF), focusing lens (FL), xyz control stage, sample cell and stage, beam block (BB, magnified in inset), iris, off-axis parabolic mirror (OAP), time-delay compensator (TDC), phase-shifting unit (PSU), two 50 mm quartz wafers (QW), polarizer analyzer (PA), band-pass filter (BPF), and photomultiplier tube (PMT). The fundamental 1030 nm is depicted in red, and the solid green is the second harmonic produced from the sample (SI). The short-dashed green line represents the LO field and the long-dashed green line represents the RO field.

Figure 2. Validation of the SIROLO electric field triplet interferometer using bulk quartz, fused silica, and hematite. (A) s-in/p-out SHG intensity from the bulk of a 1 cm thick square block of z-cut α-quartz as a function of its azimuthal rotational angle (internal reflection geometry). (B) SILO (light blue), SIROLO (dark blue), and ROLO (black) interference fringes from a bulk quartz block collected in internal reflection as a function of PSU angle. The SHG intensity for the SILO fringe is offset by 6.6 x 10^4 and multiplied by ten. (C) SILO (light green), SIROLO (dark green), and ROLO (black) interference fringes from a fused silica:water interface at its PZC (pH

2.5, 1 M NaCl) as a function of PSU angle. (D) SILO (yellow), SIROLO (orange), and ROLO (black) interference fringes from a hematite:air interface. (E) ROLO amplitude (left ordinate) and phase (right ordinate) recorded over 18 hours, and linear least squares fit (line). Please see text for detail.

Scheme 1

A

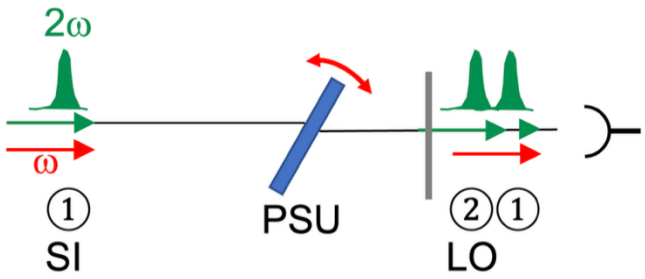

B

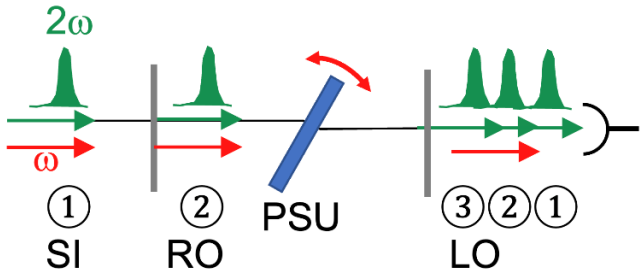

Figure 1

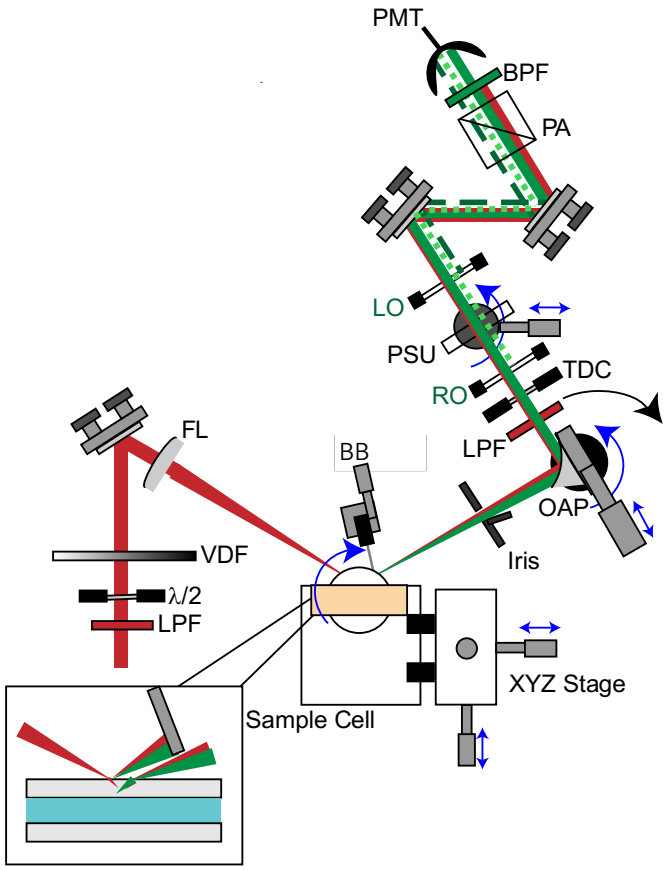
PMT
BPF
PA
LO
PSU
TDC
RO
LPF
OAP
Iris
BB
FL
VDF
λ/2
LPF
Sample Cell
XYZ Stage

Figure 2

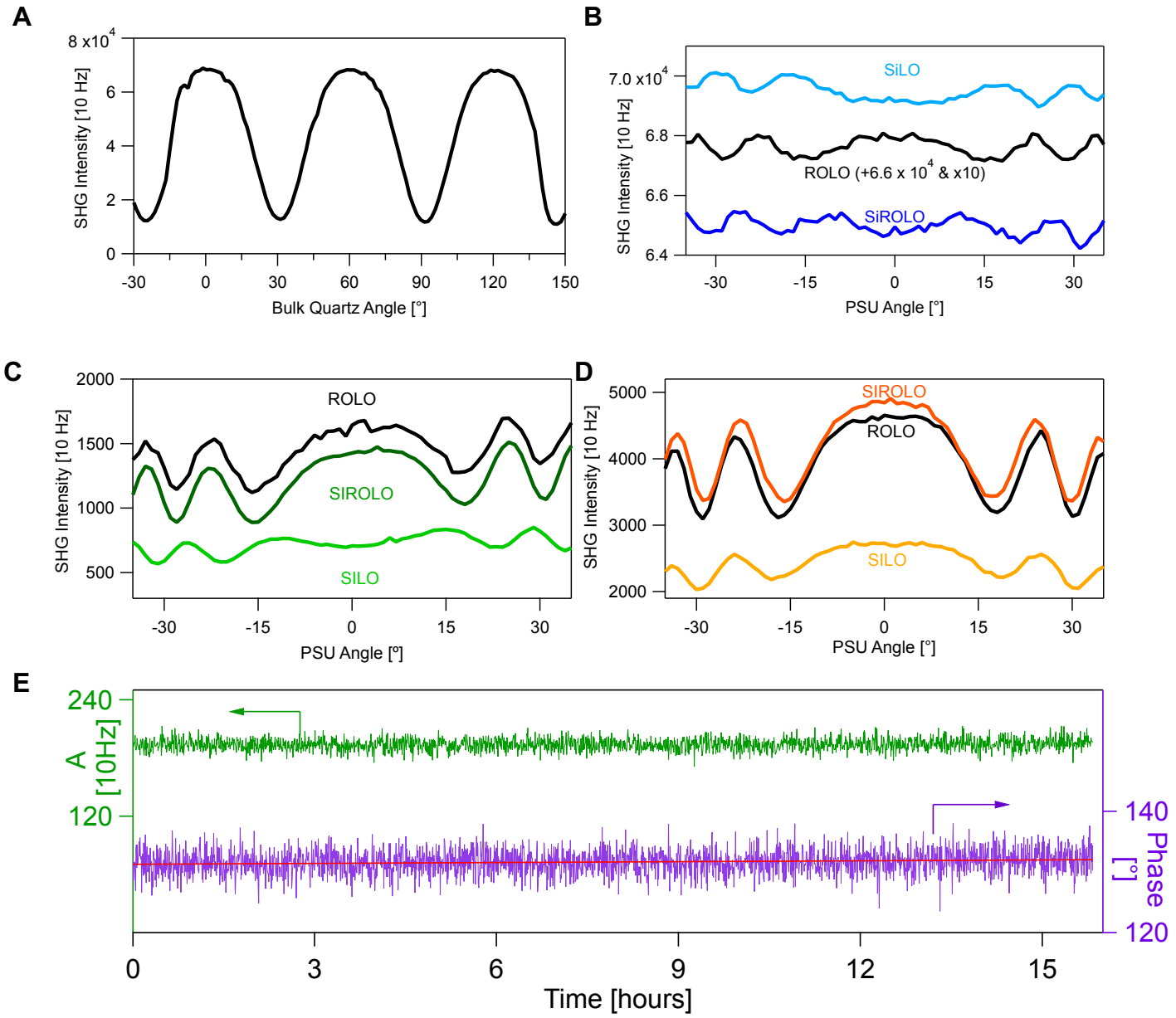
A
8 x10^4
SHG Intensity [10 Hz]
Bulk Quartz Angle [°]
B
7.0 x10^4
SiLO
ROLO (+6.6 x 10^4 & x10)
SiROLO
SHG Intensity [10 Hz]
PSU Angle [°]
C
ROLO
SIROLO
SILO
SHG Intensity [10 Hz]
PSU Angle [°]
D
SIROLO
ROLO
SILO
SHG Intensity [10 Hz]
PSU Angle [°]
E
A [10Hz]
Phase [°]
Time [hours]